Research *Ünal vd.,/Kırklareli University Journal of Engineering and Science 8-2 (2022) 273-288*
DOI: 10.34186/klujes.1178165 *Geliş Tarihi:21.09.2022* *Kabul Tarihi:05.12.2022*

SYNTHESIS AND INVESTIGATION OF STRUCTURAL, SURFACE MORPHOLOGICAL AND OPTICAL PROPERTIES OF InSe/PMItz HYBRID HETEROJUNCTION

Fatih ÜNAL[1*], Merve ZURNACI[2], Serkan DEMİR[3], Mahmut GÜR[4], Nesrin ŞENER[5], İzzet ŞENER[6]

[1] *Central Research Laboratory, Application and Research Center, Giresun University, Giresun, Turkey*
[2] *Central Research Laboratory, Kastamonu University, Kastamonu, Turkey*
[3] *Department of Industrial Engineering, Faculty of Engineering, Giresun University, Giresun, Turkey.*
[4] *Department of Forest Industrial Engineering, Faculty of Forestry, Kastamonu University, Kastamonu, Turkey*
[5] *Chemistry Department, Faculty of Arts and Sciences, Kastamonu Uni., Kastamonu, Turkey*
[6] *Department of Food Engineering, Faculty of Engineering and Architecture, Kastamonu Uni., Kastamonu, Turkey*

Abstract

On a series of annealed and unannealed InSe thin films which were formerly produced by electrochemical deposition method, organic PMItz semiconductor compound was growth by physical vapour deposition (PVD) method. Structural analyses of the films carried out by X-ray diffractometry (XRD) method revealed that glass/ITO/InSe film formed in hexagonal InSe phase while glass/ITO/InSe(annealed) film formed in monoclinic In_6Se_7 and orthorombic In_4Se_3 phases. Surface analyses were conducted by atomic force microscoby (AFM) and it is observed that the layers are homogenous and have different roughness values. Optical analyses of the films demonstrated that annealing of the film result with increased absorption coefficient and reduced energy band gap. Moreover, other optical parameters of the films i.e. refractive indice(n), extinction coefficient (k), real dielectric constant(ε_r), imaginary dielectric constant (ε_i) and optical conductivity were determined and compared within 300-1000 nm range.

Keywords: InSe, Organic semiconductor Hybrid heterojunction, Opto-electronic.

Sorumlu yazar: Fatih ÜNAL, fatih.unal@giresun.edu.tr

Research *Ünal vd.,/Kırklareli University Journal of Engineering and Science 8-2 (2022) 273-288*
DOI: 10.34186/klujes.1178165 *Geliş Tarihi:21.09.2022* *Kabul Tarihi:05.12.2022*

InSe/PMItz HIBRIT HETEROEKLEMİNİN SENTEZİ VE YAPISAL, YÜZEYSEL VE OPTİKSEL ÖZELLİKLERİNİN İNCELENMESİ

Öz

Elektrokimyasal depolama yöntemi kullanılarak üretilen ve bir grubu tavlanan inorganik InSe ince filmlerinin üzerine fiziksel buhar depolama yöntemiyle PMItz organik yarıiletken bileşiği kaplanmıştır. İnorganik filmlerin yapısal analizi X ışınları difraktometresiyle (XRD) yapılmış, glass/ITO/InSe filminin hegzagonal InSe fazından oluştuğu görülmüşken glass/ITO/InSe(tavlanmış) filminin monoklinik In_6Se_7 ve ortorombik In_4Se_3 fazlarını içerdiği görülmüştür. Tabakaların yüzey analizi atomik kuvvet mikroskobu (AFM) ile yapılmış ve tabakaların homojen bir şekilde oluştuğu ve farklı pürüzlülük değerlerine sahip olduğu görülmüştür.

UV-Vis spektrometresiyle yapılan optiksel analiz neticesinde; tavlanmış InSe bileşiği ile oluşan heteroeklemin soğurma katsayısının arttığı ve enerji band aralığı değerlerinin azaldığı görülmüştür. Ayrıca heteroeklemlerin diğer optiksel parametreleri; refraktif indeks (n), molar zayıflama katsayısı (k), gerçek dielektrik sabit (ε_r), hayali dielektrik sabit (ε_i) ve optiksel iletkenlik (σ) hesaplanmış ve 300-1000 nm dalga boyu aralığında bu değerler karşılaştırılmıştır.

Anahtar Kelimeler: InSe, Organik yarıiletken, Hibrit heteroeklem, Opto-elektronik.

1. INTRODUCTION

In modern optoelectronic devices which are critical both industrial and commercial applications, inorganic thin film semiconductors play key roles because of their intrinsic electronic structural characteristics that give rise to their uses as absorber layer, window layer, substrate and so on. Among them, Indium Selenides (In_xSe_y) come forwards in last few decades with respect to other III-VI compounds owing to their unusual electronic structures, inherent polymorphism and involving of different stoichiometries [1-7]. Different stoichiometric combinations of In_xSe_y provide adjustment of band gap and dangling covalent bonds at their layered surface allow heterojunction with other types of organic or inorganic semiconductor [8-10]. Conversely, owing to their rigid physical structure and relatively high fabrication costs, variation of these types inorganic thin films is unfortunately limited. At this point, heteroepitaxy of inorganic materials

DOI: 10.34186/klujes.1178165 Geliş Tarihi:21.09.2022 Kabul Tarihi:05.12.2022

with organic small molecules by various methods improves this drawback by increasing the diversity of devices and eliminating the above disadvantages since organic thin film semiconductors are of more flexible film structure, tunable opto-electronic properties by molecular modulation and their fabrication is more affordable [11-15]. As one of the most popular organic semiconductor class of materials, imidazo-phenanthrenes/-phenanthrolines are frequently used in the fabrication of advanced organic optoelectronics since past few decades. By molecular modification, their superior photophysical and electroluminescent properties can be also tuned as well as their diversities can be increased [16-22]. However, their heterojunction with inorganic thin films are still extremely rare. Our study herein reports structural and optical properties of a new heterojunction which is fabricated from In_xSe_y as substrate and a imidazophenanthrene derivative (PMItz) as absorber layer. Heteroepitaxial growth of PMItz on In_xSe_y was performed succesfully by physical vapour deposition (PVD) method.

2. MATERIALS AND METHOD

2.1. Experimental Details

Autolab PGSTAT128N model electrochemical impedance spectrometer was used for electrochemical deposition. A Vaksis PVD-MT/2M2T thermal vaporization thin film deposition system was used for thermal deposition. XRD analyses was carried out by a GNR Europe powder XRD enstrument using Cu K-α radiation with λ=1.5406 Å and in 2θ=0-70 range. AFM analyses were performed with a NANOSURF C300 model AFM instrument, at room temeprature, using top 190A1-G centilever, in dynamic force mode and within 25x25 µm scan area. Optical analyses were performed using a Thermo SCIENTIFIC Evolution Array UV-Vis spectrometer.

2.2. Construction of Glass/ITO/InSe and Glass/ITO/InSe(annealed) thin films

Epitaxial growth of In_xSe_y was taken place on a glass/ITO substrate with a specific resistance of lower than 20 Ω by using electrochemical deposition method. The conductive glass/ITO substrate is considered as a working electrode in the electrochemical deposition method. In addition, the transparency of the ITO layer does not affect the optical properties of the heterojunctions. The glass/ITO substrate was successively cleaned with deionized water, acetone, propanol and dried

DOI: 10.34186/klujes.1178165 Geliş Tarihi:21.09.2022 Kabul Tarihi:05.12.2022

with nitrogen before further deposition process 250 mM $InCl_3$ (sigma aldrich %99,999) as indium source, 250 mM H_2O_3Se (sigma aldrich %98) for as selenium source, 250 mM LiCl (sigma aldrich %99) and 350 mM KCl (sigma aldrich %99) as buffer solutions were used. For one-step electrochemical deposition, electrolyte volume was set to 60 ml using 15 ml of each solution. The pH of the electrolyte was adjusted to 1,5 with 9,45 M HCl solution and applied voltage was set to -0,95 V [23]. Platin plate as counter electrode with the dimensions of 1,0x1,5 cm, Ag/AgCl reference electrode, and glass/ITO as working electrode with the surface area of 1 cm^2 were used. The reaction was taken place at room temeprature for 60 min. and under nitrogen atmosphere with 0.1 bar. An another set of obtained films was annealed at 70 cmHg and 105 ^oC temperature during 60 min.

2.3. Fabrication of Glass/ITO/InSe/PMItz and Glass/ITO/InSe(annealed)/PMItz heterjunctions

PMItz as organic layer in powder form was growth on Glass/ITO/InSe and Glass/ITO/InSe(annealed) by PVD method. The temperature and pressure of the chamber was set to 26 ^oC and 10^{-6} torr respectively using Mo pot. Figure 1 shows the schematic representation of heterojunctions.

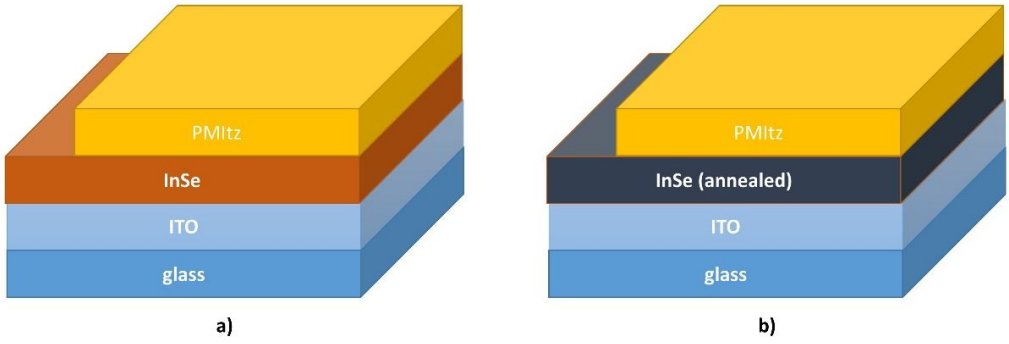

Figure 1. Schematic representation of a) glass/ITO/InSe/PMItz, b) glass/ITO/InSe(annealed)/PMItz heterjunctions

DOI: 10.34186/klujes.1178165 Geliş Tarihi:21.09.2022 Kabul Tarihi:05.12.2022

3. RESULT AND DISCUSSION

3.1. Sutructural Analyses

XRD patterns of Glass/ITO/InSe and Glass/ITO/InSe(annealed) thin films were given in Figure 2. Glass/ITO/InSe thin film consists of hexagonal InSe phase with the parameters (entry:00-034-1431) P63/mmc (194) a=4.005000 A, c=16.639999 A, Z=4 while annealed one consists of two phases where orthorombic In_4Se_3 phase with the parameters Pnnm (58) a=15.296000A, b=12.308000A, c=4.080600A Z=4 and monoclinic In_6Se_7 phase with the parameters P21(4) a=4.430000A, b=4.063000, c=18.378000A, β=109.339996o Z=2 coexist. With annealing, hexagonal InSe phase transformed into monoclinic In_6Se_7 and orthorombic In_4Se_3 phases. It was observed that InSe phase grown on (002), (004), (103), (105) planes with 2θ values of 10.63, 21.24, 30.43, 37.45. In the annealed thin film, In_6Se_7 phase grown on (201), (-105), (-212), (204) planes with 2θ values of 22.15, 24.85, 29.25, 33.25 and In_4Se_3 phase grown on (220) plane with 2θ value of 18.49.

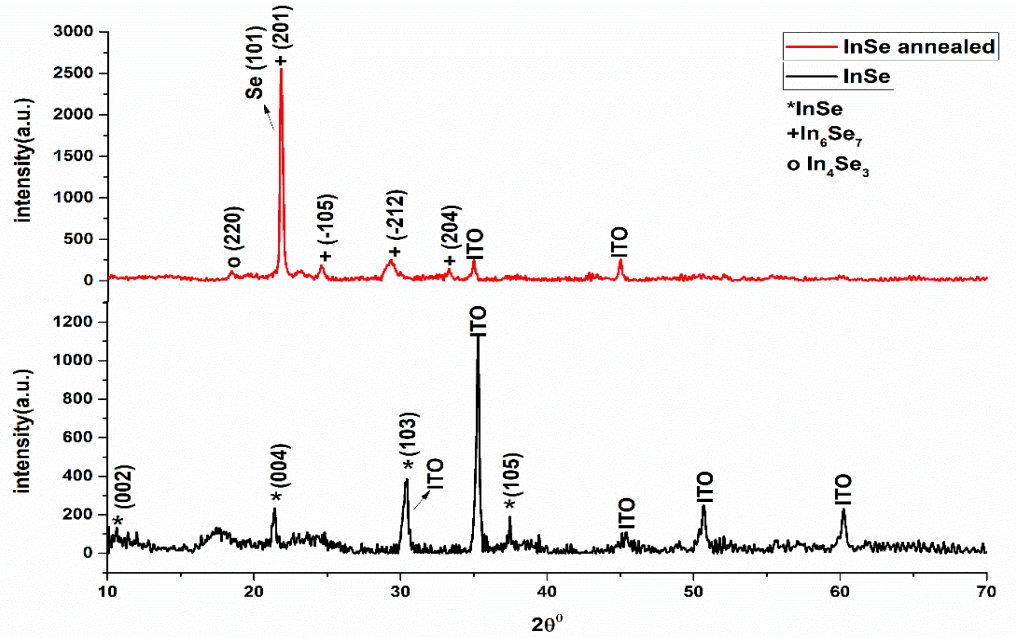

Figure 2. XRD patterns of InSe and InSe(annealed) thin films

3.2. Surface Analyses

AFM images of the fabricated thin films are given in Figures 3 and 4. It is observed that the films were homogenously deposited without any crack or hole. Table 1 lists Sa (avarage rougness) and

DOI: 10.34186/klujes.1178165 *Geliş Tarihi:21.09.2022* *Kabul Tarihi:05.12.2022*

Sq (root mean square) values of the fabricated films. According to Table 1, the roughness of the films decreased by annealing which can be ascribed to phase transition of InSe.

Table 1. Sa and Sq values of the fabricated layers

Thin film	Sa (Rougness) (nm)	Sq (Root mean square) (nm)
Glass/ITO/InSe	285.62	349.83
Glass/ITO/InSe/PMItz	253.58	302.85
Glass/ITO/InSe(annelaed)	210.78	254.09
Glass/ITO/InSe(annelaed)/PMItz	256.23	309.62

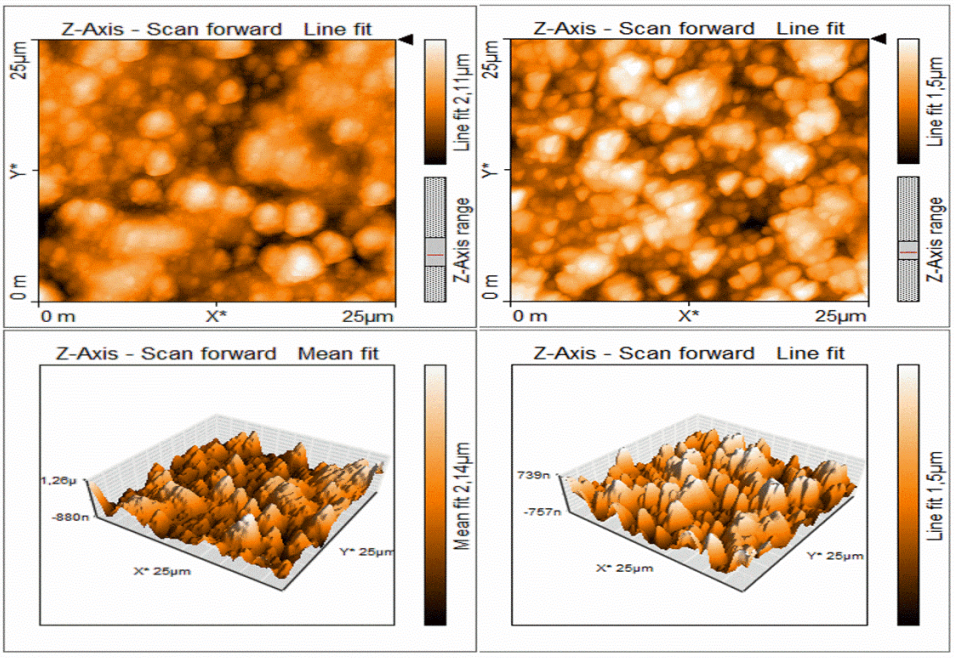

Figure 3. AFM images of Glass/ITO/InSe(left) and Glass/ITO/InSe/PMItz thin films at 25x25 µm sizes.

DOI: 10.34186/klujes.1178165 Geliş Tarihi:21.09.2022 Kabul Tarihi:05.12.2022

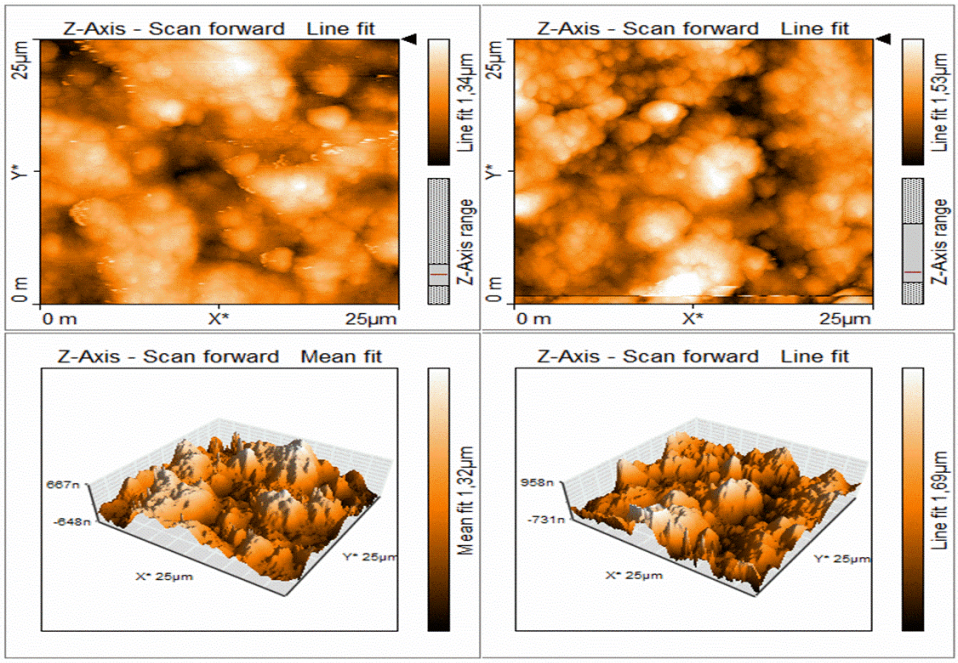

Figure 4. AFM images of Glass/ITO/InSe(annealed)(left) and Glass/ITO/InSe(annealed)/PMItz(right) thin films at 25x25 µm sizes

3.3. Optical Analyses

Absorption coefficients (α), extinction coefficients (k), transmittances (T), refractive indexes (n), optical conductivities (σ) and dielectric parameters (ε_i, ε_r, ε_i/ ε_r) of the fabricated films were calculated in 300-1000 nm range.

α is calculated from the formula [24, 25],

$$\alpha = \frac{2.303 \cdot A}{d} \quad [1]$$

Where d is thickness of the film and A is absorbance.

Energy band gap is determined by utilizing optical absorption spectroscopy technique. The relation between absorption coefficient and energy band gap (E_g) is as follow[25, 26]:

$$\alpha(h\upsilon) \approx \left(h\upsilon - E_g\right)^n \quad [2]$$

DOI: 10.34186/klujes.1178165 Geliş Tarihi:21.09.2022 Kabul Tarihi:05.12.2022

where n is equal to ½ in case of direct allowed transitions. From the plots of $(\alpha h\upsilon)^{\frac{1}{n}}$ vs hυ, E_g is determined through the extrapolation of the straight line portion of the plot to the abscissa. Thereby the intercept gives Eg.

The relation between absorbance (A) and transmittance (T) is given by;

$$A = -logT \quad [3]$$

if the multiple reflections are ignored, then the transmittance of the film is stated as [26, 27]**;**

$$T = (1-R)^2 \exp(-A) \quad [4]$$

where the reflectance R can be estimated throught the measurements of both T and A using Eq. (4) which can be reorganized as follow

$$R = 1 - \left(\frac{T}{\exp(-A)}\right)^{1/2} \quad [5]$$

The relation between absorption (α) and extinction (k) coefficients is calculated as

$$k = \frac{\lambda \cdot \alpha}{4\pi} \quad [6]$$

Then the refractive index (n) is given as[27]:

$$n = \frac{1+R}{1-R} + \sqrt{\frac{4R}{1-R^2} - k^2} \quad [7]$$

The real and imaginary parts of the dielectric constant, loss and optical conductivity are given as $\varepsilon_r = n^2 - k^2$, $\varepsilon_i = 2nk$, $\varepsilon_i / \varepsilon_r$ and $\sigma = \alpha nc/4\pi$ [28] respectively.

In Figure 5, the graphs of absorption coefficients versus wavelength is plotted for heterojunctions. Both heterojunctions have large absorption profiles and high absorption coefficients. Although As seen in Figure 5, the glass/ITO/InSe(annealed)/PMItz heterojunction exhibits higher absorption in the whole range and gives the strongest peak at 330 nm with a α value of 6.45×10^6 m^{-1}. The unannealed film gives the strongest peak at 382 nm with a α value of 5.85×10^6 m^{-1} . The annealed film gives a shoulder between 662-474 nm and the strongest peak at 330 nm with a α value of 6.45×10^6 m^{-1}. As expected, the strengthening of absorption profile upon anneraling can be dedicted to phase transition of InSe. The plot of hυ versus $(\alpha h\upsilon)^2$ is given in Figure 4 (right). Direct band gap of PMItz which was deposited on InSe phases was previously calculated in our previous report [29]. It is observed that both heterojunctions have two energy band gap then. The forbidden band

DOI: 10.34186/klujes.1178165 Geliş Tarihi:21.09.2022 Kabul Tarihi:05.12.2022

gaps of unannealed and glass/ITO/InSe(annealed)/PMItz heterojunctions were calculated to be 2.75 eV, 2.11eV and 2.63eV, 1.66eV respectively, which are in visible range. The decrease of forbidden band gap is due to the change in the structure of the inorganic layer by annealing [30]. In addition, it was observed that Eg values were lower than coronene/ZnO [28], Cu doped ZnO/coronene [31] heterojunctions.

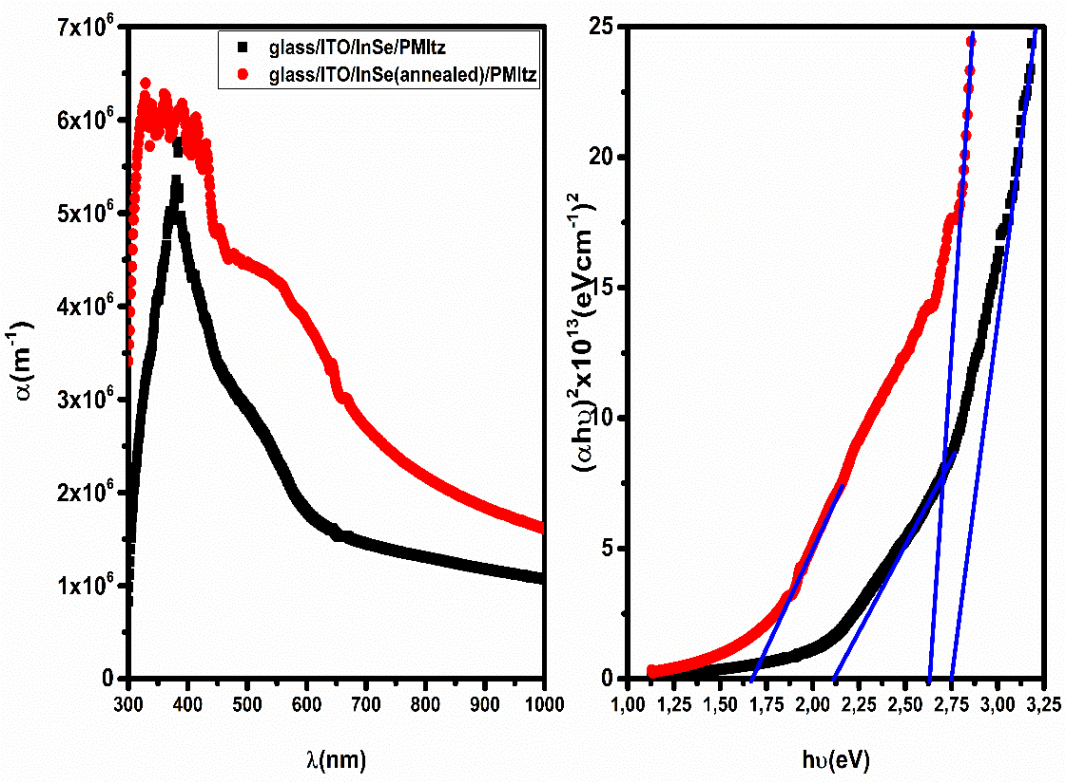

Figure 5. Absorption coefficients versus. λ(left) and hυ versus. $(\alpha h\upsilon)^2$ (right) plots of glass/ITO/InSe/PMItz and glass/ITO/InSe(annealed)/PMItz heterojunctions.

Figure 6 represents plots of T% and R% versus λ for glass/ITO/InSe/PMItz and glass/ITO/InSe(annealed)/PMItz heterojunctions. Transmittance of glass/ITO/InSe/PMItz heterojunction is 19.2% while that of glass/ITO/InSe(annealed)/PMItz heterojunction one is 12.93%. The transmittance reduced down to 0.04 in absorption region and denotes to strong absorption of the films. In similar to situation observed in absorption region, glass/ITO/InSe(annealed)/PMItz heterojunction exhibited lower transmittance than

DOI: 10.34186/klujes.1178165 Geliş Tarihi:21.09.2022 Kabul Tarihi:05.12.2022

glass/ITO/InSe/PMItz one. R% values rised up to absorption region from 1000 nm and decreased down to lower wavelengths than absorption region.

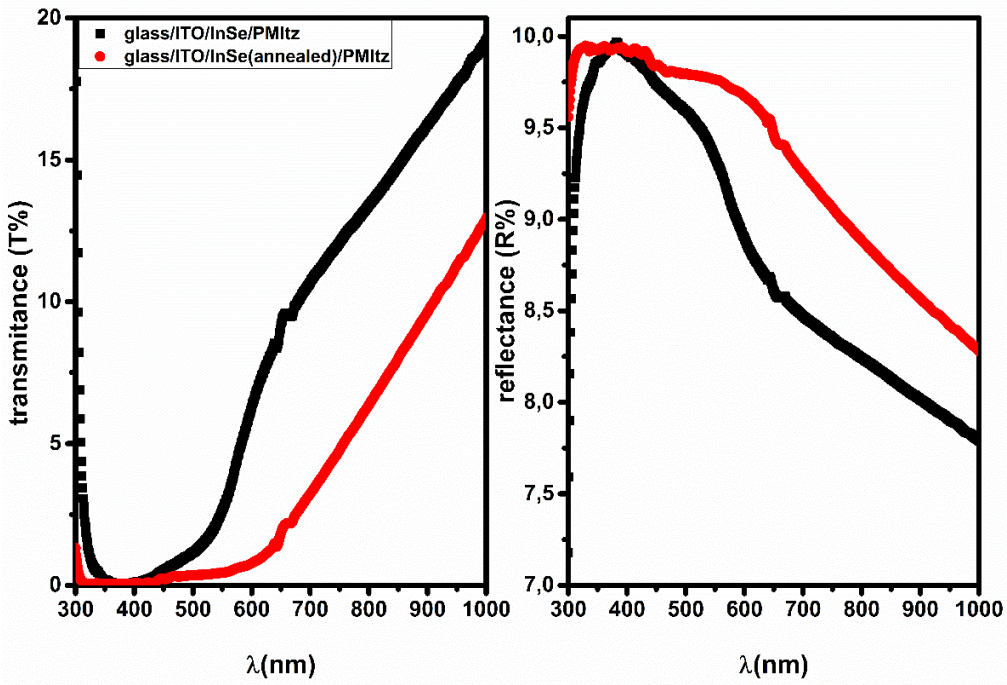

Figure 6. λ versus transmittance% (left) and reflectance% (right) plots of glass/ITO/InSe/PMItz and glass/ITO/InSe(annealed)/PMItz heterojunctions.

The plots of k and n values versus nm are given in Figure 7. As clearly seen in Figure 7(left), the glass/ITO/InSe(annealed)/PMItz heterojunction has higher k values than glass/ITO/InSe/PMItz heterojunction one. The higher k value indicates that more quenching of incident light take place, which means it is absorbed by the material. The n values of glass/ITO/InSe(annealed)/PMItz heterojunction are higher down to 550 nm while the opposite trend is observed in 550-350 nm range. Maximum n values for glass/ITO/InSe(annealed)/PMItz and glass/ITO/InSe/PMItz heterojunction are 1.46 and 1.47 respectively, which are higher than our previously fabricated hterojunctions [29].

DOI: 10.34186/klujes.1178165 *Geliş Tarihi:21.09.2022* *Kabul Tarihi:05.12.2022*

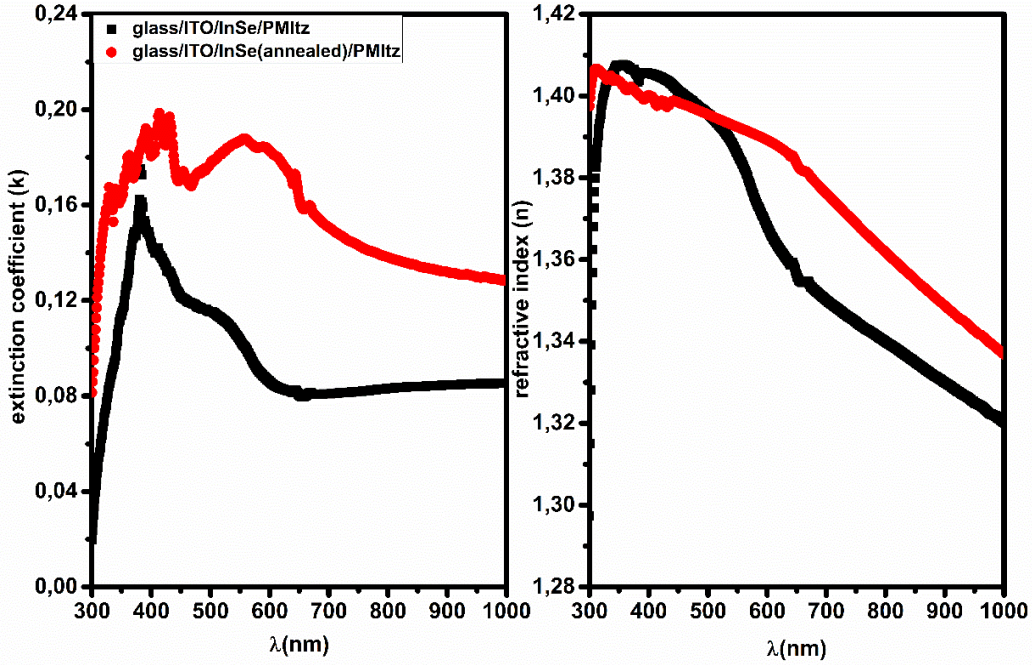

Figure 7. The plots of k(left) and n(right) versus nm for glass/ITO/InSe/PMItz and glass/ITO/InSe(annealed)/PMItz heterojunctions.

Figure 8 represents ln(α) versus hυ graphs of heterojunctions. The spectral dependence in the edge of absorption is given by the Urbach or band tail energy (Eu). According to the Urbach energy, the band tails of the localized states are in correlation with the microstructural lattice disorders, and the crystal defects can be estimated according to following equation [32]

$$\alpha = \alpha_0 \exp\left(\frac{h\upsilon}{E_U}\right) \quad [8]$$

E_U values of glass/ITO/InSe(annealed)/PMItz and glass/ITO/InSe/PMItz heterojunctions are respectively 0.26 eV and 0.54 eV which can be calculated from the inverse of slope of th graph. The decrease of E_U means reducing of intrinsic disorder [33]. Namely, PMItz has more organized atomic rearrangement on annealed InSe structure and it can be noticed from AFM analyses. E_U is also inversely associated with the crystal size of the structure and hence E_U of PMItz is low owing to big crystal size of organic structure [32, 34].

DOI: 10.34186/klujes.1178165 *Geliş Tarihi:21.09.2022* *Kabul Tarihi:05.12.2022*

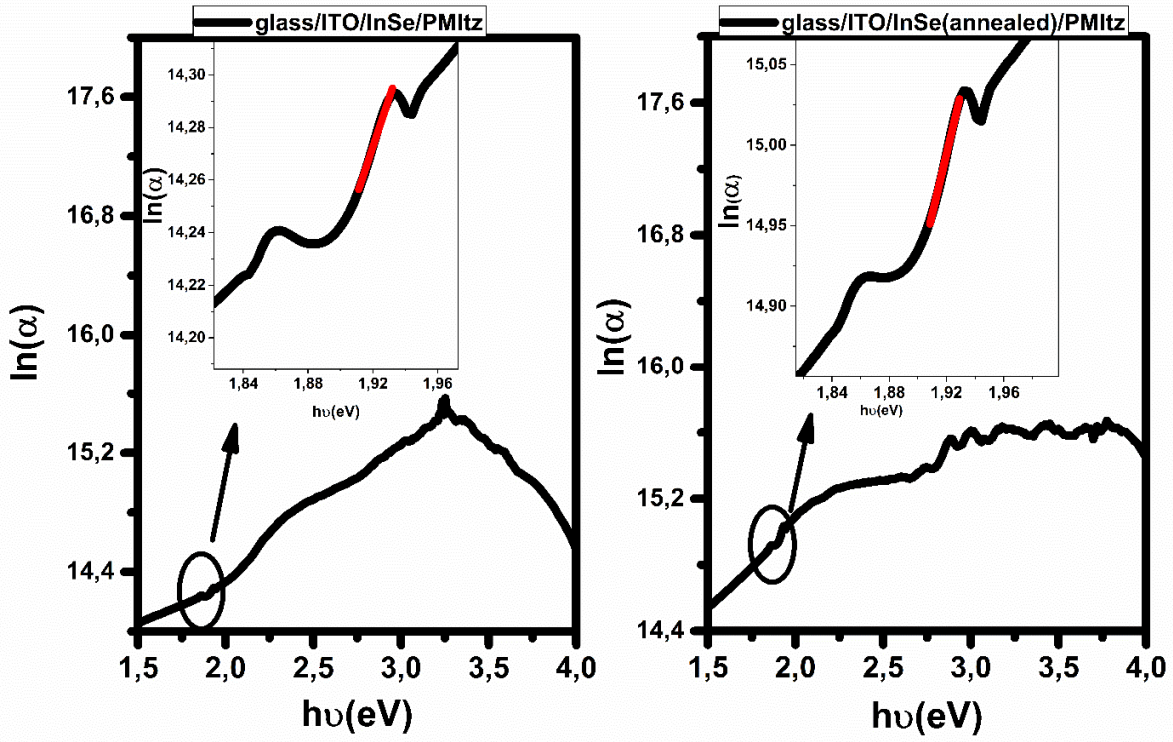

Figure 8. hυ versus ln(α) graphs of glass/ITO/InSe/PMItz (left) and glass/ITO/InSe(annealed)/PMItz (right) heterojunctions.

Real and imaginary dielectric constants vs hυ plots are depicted in Figure 9. In both heterojunctions, real part of dielectric seems higher than imaginary one. Real dielectric constants increased for both heterojunction with increasing energy of incident light while imaginary dielectric constant increased up to absorption region and decreased after. Figure 10 shows the graph of optical conductivity and dielectric loss versus hυ. Glass/ITO/InSe(annealed)/PMItz heterojunction exhibits higher optical conductivity than unannealed one. Nevertheless, the values are reasonably higher than even our previously reported heterojunction where PMItz was growth only on ITO. Also dielectric loss value of glass/ITO/InSe(annealed)/PMItz heterojunction is higher than that of glass/ITO/InSe/PMItz heterojunction one.

DOI: 10.34186/klujes.1178165 *Geliş Tarihi:21.09.2022* *Kabul Tarihi:05.12.2022*

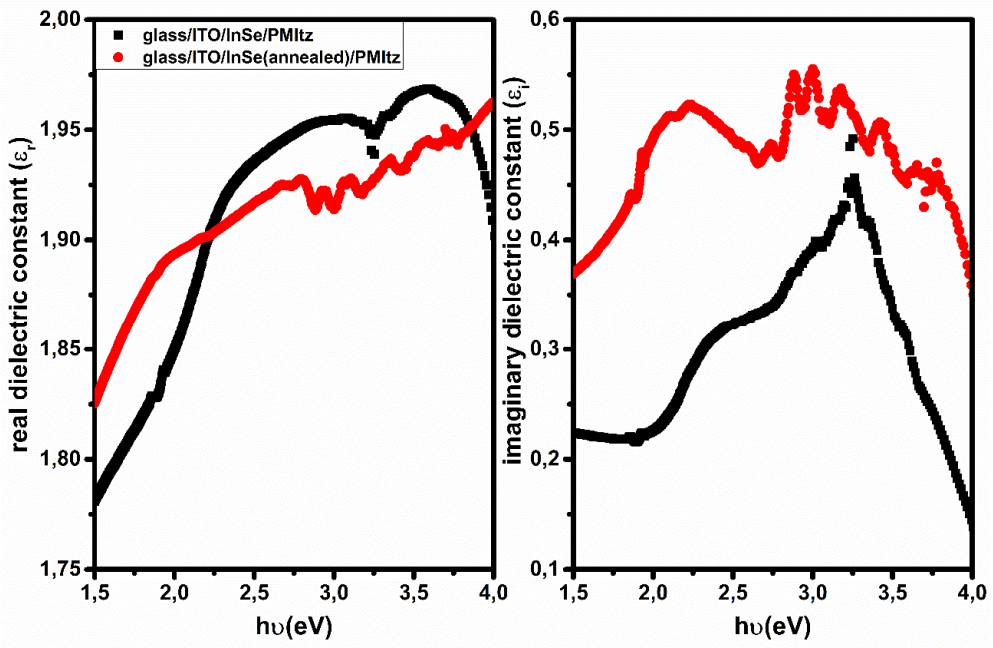

Figure 9. the real(left) and imaginary(right) parts of dielectic functions versus hυ for glass/ITO/InSe/PMItz and glass/ITO/InSe(annealed)/PMItz heterojunctions.

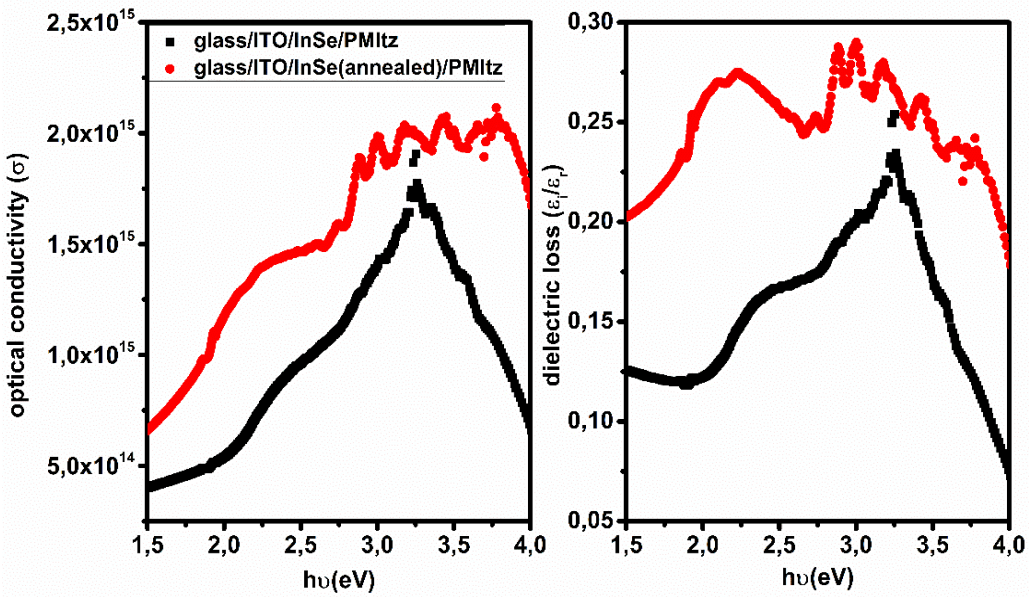

Figure 10. Optical conductivity(left) and dielectric loss(right) versus hυ for glass/ITO/InSe/PMItz and glass/ITO/InSe(annealed)/PMItz heterojunctions.

DOI: 10.34186/klujes.1178165 Geliş Tarihi:21.09.2022 Kabul Tarihi:05.12.2022

4. CONCLUSION

InSe thin films were obtained succesfully on to glass/ITO substrate by electrochemical deposition method. By annealing, stoichiometric change of InSe was determined by XRD analyses. Organic PMItz semiconductor was deposited on the obtained thin films by PVD method. Thereby, glass/ITO/InSe/PMItz and glass/ITO/InSe(annealed)/PMItz hybrid heterjunctions were fabricated. Surface analyses of the films revealed homogeneity of the them while PMItz layers are more rougher. Optical analyses data of the films demonstrated that optical absorption coefficients are considerably high and transmittances in visible region are very low. It is confirmed from Urbach energy calculation that atomic disorder state of the glass/ITO/InSe(annealed)/PMItz device is better. According to calculated important optical parameters (n, k, σ, ε_r, ε_r etc.), annealing procedure improves the optical properties of the devices.

REFERENCES

[1] Mudd, G.W., et al., Tuning the Bandgap of Exfoliated InSe Nanosheets by Quantum Confinement. Advanced Materials, 2013. 25(40): p. 5714-+.

[2] Han, G., et al., Indium Selenides: Structural Characteristics, Synthesis and Their Thermoelectric Performances. Small, 2014. 10(14): p. 2747-2765.

[3] Yuksek, M., et al., Nonlinear and saturable absorption characteristics of Ho doped InSe crystals. Optics Communications, 2014. 310: p. 100-103.

[4] Ho, C.H. and Y.J. Chu, Bending Photoluminescence and Surface Photovoltaic Effect on Multilayer InSe 2D Microplate Crystals. Advanced Optical Materials, 2015. 3(12): p. 1750-1758.

[5] Politano, A., et al., Indium selenide: an insight into electronic band structure and surface excitations. Scientific Reports, 2017. 7.

[6] Zhou, J.D., et al., InSe monolayer: synthesis, structure and ultra-high second-harmonic generation. 2d Materials, 2018. 5(2).

[7] Fatih, Ü., et al., Electrical Properties of InSe/PMItz Nanocomposite Thin Films. Journal Of Materials And Electronic Devices, 2022. 3(1).

[8] Wang, Y., et al., Molecular Doping of 2D Indium Selenide for Ultrahigh Performance and Low-Power Consumption Broadband Photodetectors. Advanced Functional Materials, 2021. 31(30).

[9] Sanchez-Royo, J.F., et al., Electronic structure, optical properties, and lattice dynamics in atomically thin indium selenide flakes. Nano Research, 2014. 7(10): p. 1556-1568.

DOI: 10.34186/klujes.1178165 Geliş Tarihi:21.09.2022 Kabul Tarihi:05.12.2022

[10] Cho, S.H., et al., Bias-controlled multi-functional transport properties of InSe/BP van der Waals heterostructures. Scientific Reports, 2021. 11(1).

[11] Zhou, Y., Optoelectronic Organic–Inorganic Semiconductor Heterojunctions. 1st ed, ed. Y. Zhou. 2021: CRC Press. 351.

[12] Wang, Z., L. Huang, and L. Chi, Organic Semiconductor Field-Effect Transistors Based on Organic-2D Heterostructures. Frontiers in Materials, 2020. 7(295).

[13] Novota, M., et al., New phenanthrene-based organic semiconductor material for electronic devices. 2014 10th International Conference on Advanced Semiconductor Devices & Microsystems (Asdam), 2014: p. 97-100.

[14] Pudasaini, P.R. and A.A. Ayon, Low-cost, high-efficiency organic/inorganic hetero-junction hybrid solar cells for next generation photovoltaic device. 13th International Conference on Micro and Nanotechnology for Power Generation and Energy Conversion Applications (Powermems 2013), 2013. 476.

[15] Li, G.W., et al., Planar Conjugated Polymers Containing 9,10-Disubstituted Phenanthrene Units for Efficient Polymer Solar Cells. Macromolecular Rapid Communications, 2014. 35(12): p. 1142-1147.

[16] Jayabharathi, J., P. Ramanathan, and V. Thanikachalam, Synthesis and optical properties of phenanthromidazole derivatives for organic electroluminescent devices. New Journal of Chemistry, 2015. 39(1): p. 142-154.

[17] Zhuang, S.Q., et al., Efficient nondoped blue organic light-emitting diodes based on phenanthroimidazole-substituted anthracene derivatives. Organic Electronics, 2012. 13(12): p. 3050-3059.

[18] Sun, Y.F., et al., The synthesis, two-photon absorption and blue upconversion fluorescence of novel, nitrogen-containing heterocyclic chromophores. Dyes and Pigments, 2009. 81(1): p. 10-17.

[19] Wang, B., et al., Pyridine-containing phenanthroimidazole electron-transport materials with electron mobility/energy-level trade-off optimization for highly efficient and low roll-off sky blue fluorescent OLEDs. Journal of Materials Chemistry C, 2015. 3(29): p. 7709-7719.

[20] Chen, W.C., et al., Molecular modification on bisphenanthroimidazole derivative for deep-blue organic electroluminescent material with ambipolar property and high performance. Organic Electronics, 2015. 17: p. 159-166.

[21] Li, C.L., et al., High performance full color OLEDs based on a class of molecules with dual carrier transport channels and small singlet-triplet splitting. Chemical Communications, 2015. 51(53): p. 10632-10635.

[22] Wang, Z.M., et al., Phenanthro[9,10-d]imidazole as a new building block for blue light emitting materials. Journal of Materials Chemistry, 2011. 21(14): p. 5451-5456.

DOI: 10.34186/klujes.1178165 Geliş Tarihi:21.09.2022 Kabul Tarihi:05.12.2022

[23] Ünal, F., ITO cam üzerine büyütülen InSe/rubrene, CIS/rubrene, CIGS/rubrene, InSe/coronene, CIS/coronene, CIGS/coronene heteroeklemlerin yapısal, optik ve elektriksel özelliklerinin belirlenmesi. 2021.

[24] AktaŞ, S. and F. ÜNal, Investigation of Structural and Electrical Properties of Metal Oxide and Organic Based Multi Heterojunction. Karadeniz Fen Bilimleri Dergisi, 2022. 12(1): p. 508-520.

[25] ÜNAL, F., Investigation Of Some Optical And Electrical Properties Of InSe Thin Film, a Window Layer for Photovoltaic Cell Growth on Glass/GaSe Substrate by M-CBD Method. Karadeniz Fen Bilimleri Dergisi, 2021. 11(1): p. 297-306.

[26] Dwivedi, D.K., et al., Structural and optical investigations of Cd1-xZnxTe thin film. Journal of Non-Crystalline Solids, 2010. 356(31-32): p. 1563-1568.

[27] Kırmızıgül, F., E. Güneri, and C. Gümüş, Effects of different deposition conditions on the properties of Cu2S thin films. Philosophical Magazine, 2013. 93(5): p. 511-523.

[28] Kurt, M.S., et al., Optical and Electrical Characterization of a ZnO/Coronene-Based Hybrid Heterojunction Photodiode. Journal of Electronic Materials, 2022.

[29] Zurnacı, M., et al., Synthesis of a new 1,3,4-thiadiazole-substituted phenanthroimidazole derivative, its growth on glass/ITO as a thin film and analysis of some surface and optoelectronic properties. New Journal of Chemistry, 2021. 45(48): p. 22678-22690.

[30] Unal, F., S. Demir, and H. Mammadov, Structural, surface morphological, optical and electrical properties of InxSey thin films, an absorber layer for photovoltaic cells fabricated by M-CBD method using different variables. Turkish Journal of Chemistry, 2021. 45(6): p. 1761-1773.

[31] Aktas, S., et al., Fabrication and morphological, optical, and electrical characterisation of Cu-doped ZnO nanorod/coronene nanowire hybrid heterojunctions. Physica Scripta, 2022.

[32] Norouzzadeh, P., et al., Investigation of structural, morphological and optical characteristics of Mn substituted Al-doped ZnO NPs: A Urbach energy and Kramers-Kronig study. Optik, 2020. 204: p. 164227.

[33] OLeary, S.K., S. Zukotynski, and J.M. Perz, Disorder and optical absorption in amorphous silicon and amorphous germanium. Journal of Non-Crystalline Solids, 1997. 210(2-3): p. 249-253.

[34] Pandey, P., R. Kurchania, and F.Z. Haque, Structural, diffused reflectance and photoluminescence study of cerium doped ZnO nanoparticles synthesized through simple sol–gel method. Optik, 2015. 126(21): p. 3310-3315.